Constitutive Modeling of Material Damage for Fatigue Failure Prediction

C. L. CHOW* AND Y. WEI
Department of Mechanical Engineering
University of Michigan-Dearborn
Dearborn, MI 48128-1491

ABSTRACT: This paper presents a constitutive modeling of material damage capable of characterizing fatigue damage and plastic damage for rate-independent materials under multiaxial loading with the theory of damage mechanics. First, an internal state variable known as the damage variable is introduced with two scalars to characterize material degradation due to the change of material microstructures under fatigue. Then, depending upon the level of applied stress in a material element, the damage accumulation is postulated to undergo two processes, the accumulation of fatigue damage and plastic damage. Two surfaces, fatigue damage surface and plastic damage surface, are proposed to quantify fatigue damage initiation and plastic damage initiation. The damage-coupled constitutive equations of elasticity and plasticity plus two corresponding damage evolution equations are formulated based on the irreversible thermodynamics. Finally, a failure criterion based on the overall damage accumulation is postulated to govern crack initiation and propagation in material elements.

A test program to determine the necessary material parameters is also provided. These parameters are considered intrinsic material properties required as the finite element input for predicting damage accumulation under fatigue loading. As an example, experiments are carried out to measure a set of damage parameters for aluminum alloy 2024-T3. The measured parameters are then used to demonstrate systematically how the damage parameters can be effectively evaluated.

KEY WORDS: damage mechanics, fatigue failure, fatigue damage, plastic damage, damage surface, constitutive modeling, irreversible thermodynamics, AL 2024-T3.

1. INTRODUCTION

METAL FATIGUE IS a complex phenomenon especially when irreversible plastic deformation is involved. The complexity of fatigue behavior under multiaxial loading is well demonstrated by the fact that although numerous investigators

*Author to whom correspondence should be addressed.

1056-7895/99/04 0355–21 $10.00/0

have worked in this field and proposed various methods of analysis [1–11], there is still a lack of a satisfactory theory of general applicability. Despite its popularity, the limitations and anomalies associated with the use of the S-N curve for engineering design analysis are well recognized and acknowledged by engineers and scientists alike. This is primarily due to the complex microstructure evolution during loading process which is difficult to accurately describe and model with conventional approaches by assuming materials free of micro-defects, especially when irreversible plastic deformation is involved. Nevertheless, different failure criteria were introduced for a failure process: one is centered on the S-N curve for specimens without macro-cracks, and the other is the fracture mechanics methodology for specimens with macro-cracks. However, such a distinction is not based on sound reasoning or physical behavior and is considered arbitrary. Metal fatigue can therefore be regarded as the least developed branch of engineering mechanics. Consequently, costly failures of industrial plant and equipment still occur today.

Metal fatigue may be considered as a form of material degradation/damage caused by cyclic loading. This material behavior can be well characterized with an emerging theory of damage mechanics first introduced by Kachanov [12]. This theory, based on irreversible thermodynamics, has been widely applied to study the behavior of rocks and concrete as well as ductile fracture, creep rupture and fatigue failure of metals [10,13–19]. The material degradation caused by the initiation, growth and coalescence of micro-cracks in a material element due to cyclic loading is well suited for characterization by the theory of damage mechanics.

A fatigue damage model was proposed for uniaxial cyclic loading by expressing damage accumulation rate as a function of the maximum stress, the minimum stress and the mean stress [20]. This model has been used to predict fatigue life under various loading conditions, including two-level test and block-programs [21]. Several attempts have been made to generalize this model to multiaxial loading [10]. However, two fundamental unresolved problems confront its generalization; first the definition of the multiaxial stress parameters associated with maximum, minimum and mean stress; and second the applicability of the model to complex loading, including non-proportional loading.

In this paper, a constitutive model of material damage for fatigue under multiaxial loading is developed for rate independent materials in a thermodynamic framework. The effect of hydrostatic stress on fatigue damage accumulation is taken into account by employing the concept of the damage energy release rate $\mathbf{Y}$ instead of the Von Mises stress. In Section 2, a damage variable $\mathbf{D}$ is introduced with two scalars to characterize degradation of the material integrity. Then, the corresponding conjugate thermodynamic force, known as damage energy release rate, is defined by the Helmholtz free energy. In Section 3, damage-coupled constitutive equations (elasticity and plasticity) are derived by the Helmholtz free energy and a yield function separating the elastic and elastoplastic domains in effective-stress space. In Section 4, two damage surfaces are introduced to define the fa-

tigue damage and the plastic damage domains. The damage surfaces are expressed as functions of the damage energy release rates that are used to determine the incremental forms of damage evolution equations, thus implying their applicability for non-proportional loading. In addition, a failure criterion based on the overall damage accumulation is postulated to determine the threshold condition of crack initiation and propagation for a material element. Finally, in Section 5, a test program to determine the necessary material parameters, which are considered as intrinsic material properties, is provided. As an example, experiments under monotonic tensile and cyclic loading are carried out to measure a set of parameters for aluminum alloy 2024-T3.

2. THERMODYNAMIC VARIABLES

Since the deterioration of materials as a result of the nucleation and growth of distributed micro-defects is very complex, it is necessary to introduce some averaging macro-variables (internal state variables) for computational efficiency as a practical engineering tool. The success of a damage model to a large extent depends on the definition of the damage variable that is related to the concept of effective stress. According to the damage mechanics, the effective stress tensor $\bar{\sigma}$ can be expressed in a generalized form by the Cauchy stress tensor σ as [10]

$$\bar{\sigma} = \mathbf{M}(\mathbf{D}):\sigma = (\mathbf{I} - \mathbf{D})^{-1}:\sigma \tag{1}$$

where $\mathbf{D}$ is the damage variable, $\mathbf{M}(\mathbf{D})$ is the damage effect variable and $\mathbf{I}$ is the unit tensor. In general, the damage variable $\mathbf{D}$ is a fourth rank tensor. It is always true that a fourth rank tensor can store more information and is more reasonable from the physical point of view. The inconvenience of this tensor, however, is often linked with the difficulty for the identification of material parameters and with inefficient numerical analysis. Some assumptions need to be made to simplify the form of damage variable that is guided by the experimental observations.

Due to symmetry, the stress tensor can be written as

$$\sigma^T = [\sigma_1 \quad \sigma_2 \quad \sigma_3 \quad \sigma_4 \quad \sigma_5 \quad \sigma_6] = [\sigma_{11} \quad \sigma_{22} \quad \sigma_{33} \quad \sigma_{23} \quad \sigma_{31} \quad \sigma_{12}] \tag{2}$$

Then, the variables $\mathbf{D}$ and $\mathbf{M}(\mathbf{D})$ in Equation (1) can be expressed in a form of 6×6 matrix. For the case of isotropic damage, a scalar variable D is often used to describe the state of material damage. Accordingly, the damage effect tensor $\mathbf{M}(\mathbf{D})$ and the effective stress tensor $\bar{\sigma}$ are reduced to

$$\mathbf{M}(\mathbf{D}) = \frac{1}{1 - D}\mathbf{I} \tag{3}$$

$$\bar{\sigma} = \frac{\sigma}{1 - D} \tag{4}$$

However, the isotropic damage model does not include the experimental observation that the values of Poisson's ratio of damaged materials vary with the increase of applied stress under tension loading [14,22]. The change of Poisson's ratio during a loading is often considered as a form of anisotropic damage, and should be experimentally measured. However, for most of metals, original or as-received materials may be assumed isotropic in engineering applications. This assumption is considered reasonable until damage accumulation close to the formation of macro-crack and final rupture. Therefore, it may be argued that original isotropic materials remain isotropic upon loading, although the measured values of Young's modulus and Poisson's ratio may change. Accordingly, a damage tensor **D** consisting of two scalars D_1 and D_2 is proposed as

$$\mathbf{D} = \begin{bmatrix} D_1 & D_2 & D_2 & 0 & 0 & 0 \\ D_2 & D_1 & D_2 & 0 & 0 & 0 \\ D_2 & D_2 & D_1 & 0 & 0 & 0 \\ 0 & 0 & 0 & D_1 - D_2 & 0 & 0 \\ 0 & 0 & 0 & 0 & D_1 - D_2 & 0 \\ 0 & 0 & 0 & 0 & 0 & D_1 - D_2 \end{bmatrix} \tag{5}$$

Then the damage effect tensor **M(D)** is derived by the definition in Equation (1) as

$$\mathbf{M(D)} = \frac{1}{1 - D} \begin{bmatrix} 1 & \mu & \mu & 0 & 0 & 0 \\ \mu & 1 & \mu & 0 & 0 & 0 \\ \mu & \mu & 1 & 0 & 0 & 0 \\ 0 & 0 & 0 & 1 - \mu & 0 & 0 \\ 0 & 0 & 0 & 0 & 1 - \mu & 0 \\ 0 & 0 & 0 & 0 & 0 & 1 - \mu \end{bmatrix} \tag{6}$$

where D and μ are two new scalar variables which are related to D_1 and D_2 as

$$1 - D = \frac{(1 - D_1)(1 - D_1 - D_2) - 2D_2^2}{1 - D_1 - D_2}$$

$$\mu = \frac{D_2}{1 - D_1 - D_2} \tag{7}$$

Obviously, this new damage effect tensor reduces to the typical form in Equation (3) when the scalar μ (or D_2) equals zero. Therefore, the variable μ (or D_2) can be

regarded as a damage parameter associated with change in Poisson's ratio. Accordingly, two scalars D and μ can be considered as internal state variables characterizing material damage.

For intact or undamaged materials, a specific homogenized free energy Ψ is postulated as [10]

$$\rho\Psi = W_E + \rho\Psi_P = \frac{1}{2}\sigma^T:\mathbf{C}_0^{-1}:\sigma + \rho\Psi_P(\mathbf{q}) \tag{8}$$

where ρ is the density, W_E is the elastic energy, Ψ_P is the plastic part of free energy due to strain hardening, $\mathbf{C}_0$ is the elastic tensor of the undamaged material and $\mathbf{q}$ denotes a set of internal state variables for the strain hardening. According to the principle of equivalent elastic energy that "the elastic energy of the damaged material is the same in form as that of an undamaged material except that the stress is replaced by the effective stress," the free energy for damaged materials is written by Equation (8) as [14,22]

$$\rho\Psi = \frac{1}{2}\sigma^T:\mathbf{M}^T:\mathbf{C}_0^{-1}:\mathbf{M}:\sigma + \rho\Psi_P(\mathbf{q}) = \frac{1}{2}\sigma^T:\mathbf{C}^{-1}(D,\mu):\sigma + \rho\Psi_P(\mathbf{q}) \tag{9}$$

This postulate should be understood as "no direct coupling plasticity and damaged on the free energy," but the yield surface will be affected by damage [23]. In Equation (9), $\mathbf{C}$ is the elastic tensor for damaged materials and can be derived with the aid of Equation (9) as

$$\mathbf{C}^{-1}(D,\mu) = \mathbf{M}^T:\mathbf{C}_0^{-1}:\mathbf{M} = \frac{1}{E}\begin{bmatrix} 1 & -\nu & -\nu & 0 & 0 & 0 \\ -\nu & 1 & -\nu & 0 & 0 & 0 \\ -\nu & -\nu & 1 & 0 & 0 & 0 \\ 0 & 0 & 0 & 2(1+\nu) & 0 & 0 \\ 0 & 0 & 0 & 0 & 2(1+\nu) & 0 \\ 0 & 0 & 0 & 0 & 0 & 2(1+\nu) \end{bmatrix} \tag{10}$$

E and ν known as the effective Young's modulus and Poisson's ratio respectively are the values of Young's modulus and Poisson's ratio for damaged material. The relationships of E and ν with damage variables D and μ are

$$\begin{aligned} E(D,\mu) &= \frac{E_0(1-D)^2}{1 - 4\nu_0\mu + 2(1-\nu_0)\mu^2} \\ \nu(D,\mu) &= \frac{\nu_0 - 2(1-\nu_0)\mu - (1-3\nu_0)\mu^2}{1 - 4\nu_0\mu + 2(1-\nu_0)\mu^2} \end{aligned} \tag{11}$$

E_0 and ν_0 are the values of Young's modulus and Poisson's ratio for intact or undamaged material. It is obvious from Equation (10) that the damaged material may remain isotropic, even if its Young's modulus and Poisson's ratio have changed due to increase in damage variables D and μ as shown in Equation (11). The value of Poisson's ratio remains constant when the value of μ is equal to zero. Hence, the variable μ physically represents the material damage as the result of the change in the Poisson's ratio shown in Equation (11).

The thermodynamic conjugate forces of the damage variables D and μ, known as the damage energy release rate, can be derived from the Helmholtz free energy in Equation (9) as

$$Y_D = -\rho \frac{\partial \Psi}{\partial D} = -\frac{1}{1-D}\sigma^T : \mathbf{C}^{-1} : \sigma$$
$$Y_\mu = -\rho \frac{\partial \Psi}{\partial \mu} = -\frac{1}{1-D}\sigma^T : \mathbf{A} : \sigma \tag{12}$$

where the tensor $\mathbf{A}$ can be expressed as

$$\mathbf{A}(D,\mu) = \frac{1}{E_0(1-D)}\begin{bmatrix} A_1 & A_2 & A_2 & 0 & 0 & 0 \\ A_2 & A_1 & A_2 & 0 & 0 & 0 \\ A_2 & A_2 & A_1 & 0 & 0 & 0 \\ 0 & 0 & 0 & 2(A_1 - A_2) & 0 & 0 \\ 0 & 0 & 0 & 0 & 2(A_1 - A_2) & 0 \\ 0 & 0 & 0 & 0 & 0 & 2(A_1 - A_2) \end{bmatrix} \tag{13}$$

$$A_1 = 2\mu(1-\nu_0) - 2\nu_0 \quad A_2 = (1+\mu)(1-\nu_0) - 2\mu\nu_0$$

3. CONSTITUTIVE EQUATIONS

The elastic-plastic constitutive equations coupled with damage will be derived, in this section, by the thermodynamic theory. The constitutive equation of elasticity can be derived in the true stress-true strain space by the free energy in Equation (9) as

$$\varepsilon^e = \rho \frac{\partial \Psi}{\partial \sigma} = \mathbf{C}^{-1} : \sigma \tag{14}$$

where ε^e is the true strain tensor.

For damaged materials, following Von Mises theory, the yield surface is postulated having a form expressed by the concept of the effective stress as

$$F_p(\sigma, D_p, \mu_p, R) = \sigma_p^{1/2} - [R_0 + R(p)] = 0 \tag{15}$$

where

$$\sigma_p = \frac{1}{2}\bar{\sigma}^T : \mathbf{H}_0 : \bar{\sigma} = \frac{1}{2}\sigma^T : \mathbf{H} : \sigma \quad \mathbf{H} = \mathbf{M}^T : \mathbf{H}_0 : \mathbf{M} \tag{16}$$

D_p and μ_p are plastic damage variables, $\mathbf{H}_0$ is the plastic characteristic tensor for undamaged material, $\mathbf{H}$ is the plastic characteristic tensor for damaged material, R_0 is the yield stress, p is the effective equivalent plastic strain, and R is the strain hardening threshold.

For isotropic material, the form of the tensor $\mathbf{H}_0$ is chosen as

$$\mathbf{H}_0 = \begin{bmatrix} 2 & -1 & -1 & 0 & 0 & 0 \\ -1 & 2 & -1 & 0 & 0 & 0 \\ -1 & -1 & 2 & 0 & 0 & 0 \\ 0 & 0 & 0 & 6 & 0 & 0 \\ 0 & 0 & 0 & 0 & 6 & 0 \\ 0 & 0 & 0 & 0 & 0 & 6 \end{bmatrix} \tag{17}$$

Then the form of the tensor $\mathbf{H}$ can be deduced by Equation (16) as

$$\mathbf{H} = \frac{(1-\mu_p)^2}{(1-D_p)^2}\mathbf{H}_0 \tag{18}$$

Therefore, the expression of yield surface described by Equation (15) becomes:

$$F_p(\sigma, D_p, \mu_p, R) = \frac{1-\mu_p}{1-D_p}\sigma_{eq} - [R_0 + R(p)] = 0 \tag{19}$$

where σ_{eq} is the Von Mises's stress defined as

$$\sigma_{eq} = \sqrt{\frac{1}{2}\{(\sigma_1-\sigma_2)^2 + (\sigma_1-\sigma_3)^2 + (\sigma_2-\sigma_3)^2 + 6(\sigma_4^2 + \sigma_5^2 + \sigma_6^2)\}} \tag{20}$$

$\sigma_I (I = 1,2,\ldots,6)$ are the components of true stress tensor. Similar to the conventional theory of plasticity, the constitutive equations of plasticity for damaged ma-

terials are derived in the true stress-true strain space as

$$d\varepsilon^p = \lambda_p \frac{\partial F_p}{\partial \sigma} = \frac{1-\mu_p}{1-D_p} \frac{3\mathbf{S}}{2\sigma_{eq}} \lambda_p$$
$$dp = \lambda_p \frac{\partial F_p}{\partial(-R)} = \lambda_p \tag{21}$$

where ε^p is the plastic strain tensor, $\mathbf{S}$ is the true stress deviator tensor and λ_p is a Lagrange multiplier which can be determined by means of the yield surface in Equation (19).

The relationship between the effective equivalent plastic strain increment dp and the plastic strain increment $d\varepsilon^p$ can be derived from Equation (21) as

$$dp = \frac{1-D_p}{1-\mu_p} \sqrt{\frac{2}{3} d\varepsilon^{p,T} : d\varepsilon^p} \tag{22}$$

4. DAMAGE EVOLUTION EQUATIONS

Depending upon the level of applied stress in a material element, the damage accumulation is postulated to undergo two processes, the accumulation of fatigue damage and plastic damage. Two surfaces, the fatigue damage surface $F_{fd} = 0$ corresponding to the fatigue endurance limit and the plastic damage surface $F_{pd} = 0$ corresponding to the start of plastic damage, are defined to quantify fatigue damage initiation and plastic damage initiation, respectively. Therefore, damage evolution equations can be derived in a thermodynamic framework.

4.1 Plastic Damage

The plastic damage surface is formulated with the thermodynamic conjugate forces of the plastic damage variables D_p and μ_p as

$$F_{pd}(Y_{pd}, B) = Y_{pd}^{1/2} - [B_{0p} + B(w_p)] = 0 \tag{23}$$

where Y_{pd} is postulated as

$$Y_{pd} = \frac{1}{2}(Y_{Dp}^2 + \gamma Y_{\mu p}^2) \tag{24}$$

From Equation (12), Y_{Dp} and $Y_{\mu p}$ can be defined as

$$Y_{Dp} = -\rho \frac{\partial \Psi}{\partial D_p} = -\frac{1}{1-D_p} \sigma^T : \mathbf{C}^{-1}(D_p, \mu_p) : \sigma$$
$$Y_{\mu p} = -\rho \frac{\partial \Psi}{\partial \mu_p} = -\frac{1}{1-D_p} \sigma^T : \mathbf{A}(D_p, \mu_p) : \sigma \tag{25}$$

B_{0p} is the initial plastic damage threshold, B is the plastic damage hardening, w_p is the overall plastic damage and γ is the damage evolution coefficient. In a similar way as that leading to the plastic constitutive equations, the plastic damage evolution equations are derived as

$$dD_p = -\lambda_{pd} \frac{\partial F_{pd}}{\partial Y_{Dp}} = -\frac{\lambda_{pd} Y_{Dp}}{2Y_{pd}^{1/2}}$$
$$d\mu_p = -\lambda_{pd} \frac{\partial F_{pd}}{\partial Y_{\mu p}} = -\frac{\lambda_{pd} \gamma Y_{\mu p}}{2Y_{pd}^{1/2}} \tag{26}$$
$$dw_p = \lambda_{pd} \frac{\partial F_{pd}}{\partial (-B)} = \lambda_{pd}$$

where λ_{pd} is the Lagrange multiplier which can be determined by the plastic damage surface. From Equation (23),

$$dF_{pd}(Y_{Dp}, Y_{\mu p}, B) = 0$$
$$\frac{\partial F_{pd}}{\partial Y_{Dp}} dY_{Dp} + \frac{\partial F_{pd}}{\partial Y_{\mu p}} dY_{\mu p} + \frac{\partial F_{pd}}{\partial B} \frac{dB}{dw_p} dw_p = 0$$

the Lagrange multiplier λ_{pd} can be written as

$$\lambda_{pd} = dw_p = \frac{Y_{Dp} dY_{Dp} + \gamma Y_{\mu p} dY_{\mu p}}{2Y_{pd}^{1/2} \dfrac{dB}{dw_p}} \tag{27}$$

The relationship between the overall plastic damage increment dw_p and the plastic damage variables increment dD_p and $d\mu_p$ can be derived alternatively from Equation (26) as

$$dw_p = \begin{cases} \sqrt{2\left\{(dD_p)^2 + \dfrac{1}{\gamma}(d\mu)^2\right\}}, & \text{if } \gamma \neq 0 \\ \sqrt{2}dD_p, & \text{if } \gamma = 0 \end{cases} \tag{28}$$

4.2 Fatigue Damage

For most engineering materials, the contribution of tensile stress to the fatigue damage accumulation is different from that of compressive stress due to the existence of microdefects. The different responses of these microdefects are attributed to the closure of some microcracks. In order to take into account the different damage behavior between tension and compression effects (quasi unilateral damage effect), the stress range in a cycle can be decomposed into two parts, the positive part $\Delta\sigma^+$ and the negative part $\Delta\sigma^-$, as

$$\begin{aligned} \Delta\sigma^+ &= \sigma_{max} - \sigma_0 \\ \Delta\sigma^- &= \sigma_0 - \sigma_{min} \end{aligned} \tag{29}$$

Using the stress-controlled uniaxial cyclic loading as an example for illustration, there are two cases of stress range:

1. For tension-compression loading, the minimum stress σ_{min} is negative and the value of σ_0 is zero. This means that the positive part $\Delta\sigma^+$ is the maximum stress σ_{max} and the negative part $\Delta\sigma^-$ is the absolute value of the minimum stress σ_{min}.
2. For tension-tension loading, the minimum stress σ_{min} is positive and the value of σ_0 is equal to the minimum stress. This means that the positive part $\Delta\sigma^+$ is the total stress range and the negative part $\Delta\sigma^-$ is zero.

For multiaxial cyclic loading, the stress tensor σ_0, which is used to distinguish the positive part $\Delta\sigma^+$ and the negative part $\Delta\sigma^-$, is determined by the minimum value of Y_{pd} in a cycle. Specially, if the value of Y_{pd} increases monotonically as the applied stress rises from the minimum stress to the maximum stress, the value of σ_0 equals the minimum stress and the negative part is zero. Generally, σ_{max} and σ_0 are the stress tensors corresponding to, respectively, the maximum and minimum value of Y_{pd} defined in Equation (24) over a cycle, and σ_{min} is the stress tensor at the time half a cycle before σ_{max} recurs.

A damage efficiency factor α is introduced for the unilateral damage effect and the active stress range $\Delta\sigma_{act}$ over a cycle is defined as

$$\Delta\sigma_{act} = \Delta\sigma^+ + \alpha\Delta\sigma^- \tag{30}$$

where α is the material parameter and varies from 0 to 1. It is obvious from Equation (30) that there is no contribution of the negative part on the active stress range when α equals to zero and the effect of the negative part is the same as that of the positive part if α equals to 1. Accordingly, a new stress parameter σ_{act}, called active stress, is defined in a cycle as

$$\sigma_{act} = \begin{cases} \sigma - \sigma_0 + \alpha(\sigma_0 - \sigma_{min}), & \text{if } \sigma \in [\sigma_0, \sigma_{max}] \\ \alpha(\sigma - \sigma_{min}), & \text{if } \sigma \in [\sigma_{min}, \sigma_0] \end{cases} \tag{31}$$

This active stress accounts for the difference in contributions from the positive part and the negative part. Therefore, the concept of the active stress can be used to calculate fatigue damage accumulation instead of the true stress.

The fatigue damage surface is postulated with the thermodynamic conjugate forces of the fatigue damage variables as

$$F_{fd}(Y_{fd}) = Y_{fd}^{1/2} - B_{0f} = 0 \tag{32}$$

where Y_{fd} is postulated as

$$Y_{fd} = \frac{1}{2}(Y_{Df}^2 + \gamma Y_{\mu f}^2) \tag{33}$$

Y_{Df} and $Y_{\mu f}$ are defined by the active stress as

$$\begin{aligned} Y_{Df}(\sigma, D_f, \mu_f, D_p, \mu_p) &= Y_{Dp}(\sigma_{act}, D, \mu) \\ Y_{\mu f}(\sigma, D_f, \mu_f, D_p, \mu_p) &= Y_{\mu p}(\sigma_{act}, D, \mu) \end{aligned} \tag{34}$$

B_{0f} is the fatigue damage threshold corresponding to the fatigue endurance limit, Y_{Df} and $Y_{\mu f}$ are the thermodynamic conjugate forces of the fatigue damage variables D_f and μ_f, and D and μ are total damage variables. The damage variables, which are considered as internal state variables, can be written as the summation of fatigue damage and plastic damage:

$$\begin{aligned} D &= D_f + D_p \\ \mu &= \mu_f + \mu_p \end{aligned} \tag{35}$$

The equations of fatigue damage evolution are postulated to assume a similar form as that of the plastic damage evolution shown in Equations (26) and (27)

$$dD_f = -\frac{Y_{Df}}{2Y_{fd}^{1/2}} dw_f$$

$$d\mu_f = -\frac{\gamma Y_{\mu f}}{2Y_{fd}^{1/2}} dw_f \tag{36}$$

$$dw_f = \frac{Y_{Df} dY_{Df} + \gamma Y_{\mu f} dY_{\mu f}}{2Y_{fd}^{1/2} K(w_f)}$$

The function $K(w_f)$ is expressed to a first approximation as

$$K(w_f) = K_0\left(1 - \frac{w_f}{w_c}\right) \tag{37}$$

where w_f is the overall fatigue damage, w_c is the critical value of total overall damage and K_0 is the fatigue damage constant.

4.3 Damage Accumulation and Failure Criterion

Three possible cases can now be considered for any fatigue load path based on the fatigue damage surface $F_{fd} = 0$ in Equation (32) and the plastic damage surface $F_{pd} = 0$ in Equation (23).

1. For $F_{fd} < 0$: this is the case where the material is operating under the fatigue endurance limit, and there is no damage accumulation.
2. For $F_{fd} \geq 0$ and $F_{pd} < 0$: this case corresponds to the fatigue damage with negligible plastic damage accumulation. The fatigue damage accumulation per cycle can be calculated from Equation (36)

$$\frac{\Delta w_f}{\Delta N} = \int_{\sigma_c}^{\sigma_{max}} dw_f \quad \frac{\Delta D_f}{\Delta N} = \int_{\sigma_c}^{\sigma_{max}} dD_f \quad \frac{\Delta \mu_f}{\Delta N} \int_{\sigma_c}^{\sigma_{max}} d\mu_f \tag{38}$$

   where σ_{max} is the maximum stress in a cycle and σ_c is the stress tensor determined by the fatigue damage surface $F_{fd}(\sigma_c) = 0$ in Equation (32).
3. For $F_{pd} = 0$: this case includes both fatigue damage and plastic damage accumulation. The total damage incurred in a material element is defined as the summation of fatigue damage and plastic damage. Then the total damage accumulation per cycle can be calculated from Equations (26) and (36)

$$\frac{\Delta w}{\Delta N} = \frac{\Delta w_f}{\Delta N} + \frac{\Delta w_p}{\Delta N} = \int_{\sigma_c}^{\sigma_{max}} dw_f + \int_{\sigma_d}^{\sigma_{max}} dw_p$$

$$\frac{\Delta D}{\Delta N} = \frac{\Delta D_f}{\Delta N} + \frac{\Delta D_p}{\Delta N} = \int_{\sigma_c}^{\sigma_{max}} dD_f + \int_{\sigma_d}^{\sigma_{max}} dD_p \tag{39}$$

$$\frac{\Delta \mu}{\Delta N} = \frac{\Delta \mu_f}{\Delta N} + \frac{\Delta \mu_p}{\Delta N} = \int_{\sigma_c}^{\sigma_{max}} d\mu_f + \int_{\sigma_d}^{\sigma_{max}} d\mu_p$$

where σ_d is the stress tensor determined by the plastic damage surface $F_{pd}(\sigma_d) = 0$ in Equation (23).

The existence of a damage surface has been experimentally verified at different loading paths [19]. Therefore, a failure criterion can be proposed by using overall damage accumulation associated with the concept of plastic damage surface. Based on this criterion, a material element is said to have ruptured when the total overall damage w in the element reaches a critical value w_c.

5. DETERMINATION OF MATERIAL PARAMETERS

A general method to determine the material parameters or curves is presented in this section. In principle, all parameters of the model can be determined either by monotonic tensile tests or by stress-controlled uniaxial fatigue tests (i.e., tension-tension and tension-compression). As an example, experiments were carried out to measure a set of material parameters for aluminum alloy 2024-T3 Alclad plate with thickness 3.175 mm.

5.1 Damage Evolution Coefficient γ

This damage parameter is determined with the measured values of elastic modulus E and Poisson's ratio ν of damaged material under monotonic tensile test.

The damage variables D and μ are obtained from Equation (11) with the measured values of E and μ

$$\{2(1-\nu_0)\nu + 1 - 3\nu_0\}\mu^2 + 2(1-\nu_0-2\nu_0\nu)\mu + \nu - \nu_0 = 0 \tag{40}$$

$$(1-D)^2 = \frac{E}{E_0}\{1 - 4\nu_0\mu + 2(1-\nu_0)\mu^2\} \tag{41}$$

The positive solutions are taken for these equations because the damage variables D and μ are always positive. Under monotonic tension, the thermodynamic conju-

gate forces of the damage variables D and μ in Equation (12) can thus be evaluated as

$$Y_D = -\frac{1 - 4\nu_0\mu + 2(1-\nu_0)\mu^2}{E_0(1-D)^3}\sigma^2$$
$$Y_\mu = -\frac{2\mu(1-\nu_0) - 2\nu_0}{E_0(1-D)^2}\sigma^2 \tag{42}$$

Then, the following equation about the damage evolution coefficient γ can be deduced with Equation (26) as

$$\frac{dD}{d\mu} = \frac{Y_D}{\gamma Y_\mu} = \frac{1 - 4\nu_0\mu + 2(1-\nu_0)\mu^2}{\gamma(1-D)[2\mu(1-\nu_0) - 2\nu_0]} \tag{43}$$

The solution of Equation (43) is

$$\gamma[1-(1-D)^2] = \mu^2 - \frac{2\nu_0\mu}{1-\nu_0} + \frac{1-\nu_0-2\nu_0^2}{2(1-\nu_0)^2}\ln\left(1 - \frac{1-\nu_0}{\nu_0}\mu\right) \tag{44}$$

Therefore, the damage evolution coefficient γ can be determined using the measured data of E and ν based on Equations (40), (41) and (44). It is worth noting that only few values of Young's modulus and Poisson's ratio ν close to the failure point should be measured to determine this parameter.

For the material AL 2024-T3, the Young's modulus and the Poisson's ratio of the intact material and at its rupture point are

$$E_0 = 74{,}300 \text{ MPa} \quad \nu_0 = 0.34 \quad E = 58{,}800 \text{ MPa} \quad \nu = 0.29$$

Then, the damage evolution coefficient γ can be determined as –0.4 by Equations (40), (41) and (44).

5.2 Strain Hardening Curve $R(p)$

Under monotonic tension, the strain hardening R is derived from the yield surface in Equation (19) as

$$R = \frac{1-\mu}{1-D}\sigma - R_0 \tag{45}$$

The effective plastic strain p is derived from Equation (22) as

$$p = \int_0^{\varepsilon^p} \frac{1-D}{1-\mu} d\varepsilon^p = \int_0^{\varepsilon^p} \frac{1-D}{1-\mu} \left(d\varepsilon - \frac{d\sigma}{E} \right) \tag{46}$$

Therefore, the curve of strain hardening $R(p)$ can be obtained from the measured values of true stress-true strain and the corresponding damage variables D and μ. The corresponding values of D and μ can be calculated with the measured values of Young's modulus by Equations (41) and (44).

For the material AL 2024-T3, the measured values of Young's modulus during montonic tension is depicted in Figure 1. The damage variables D and μ can then be calculated with Equations (41) and (44) as shown in Figure 2. The true stress-true strain curve under monotonic tension is given in Figure 3 and the 0.2% yield stress R_0 is 330 MPa. Therefore, the calculated strain hardening curve $R(p)$ with Equations (45) and (46) is shown in Figure 4.

5.3 Plastic Damage Hardening Curve $B(w_p)$ and Critical Value of Overall Damage w_c

Under monotonic tension, the initial plastic damage threshold B_{0p} is calculated from the plastic damage surface with Equation (23). The calculation is based on the assumption that the plastic damage starts immediately after the applied stress exceeds the yield stress

$$B_{0p} = \{0.5(1 + 4\gamma\nu_0^2)\}^{1/2} \frac{R_0^2}{E_0} \tag{47}$$

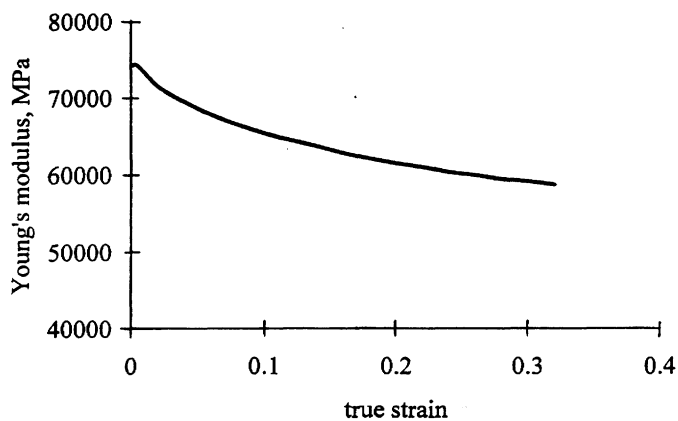

Figure 1. *The Young's modulus under monotonic tension.*

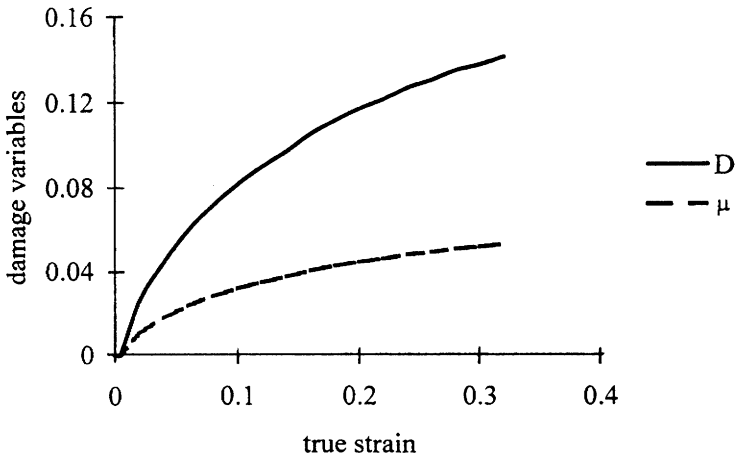

Figure 2. *The damage variables* D *and* μ *under monotonic tension.*

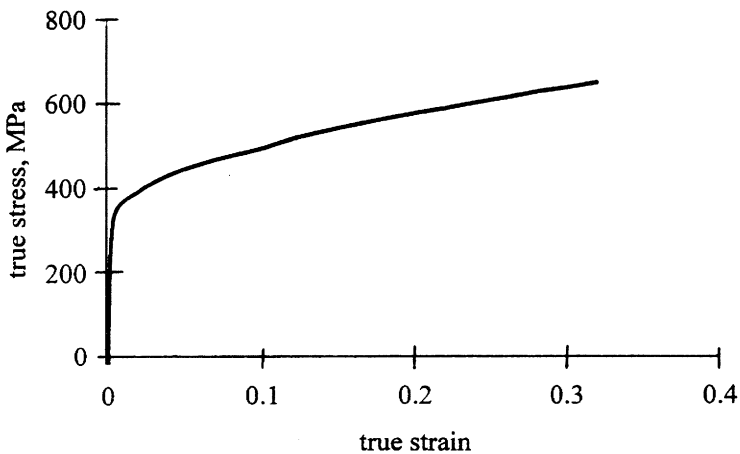

Figure 3. *True stress-true strain curve.*

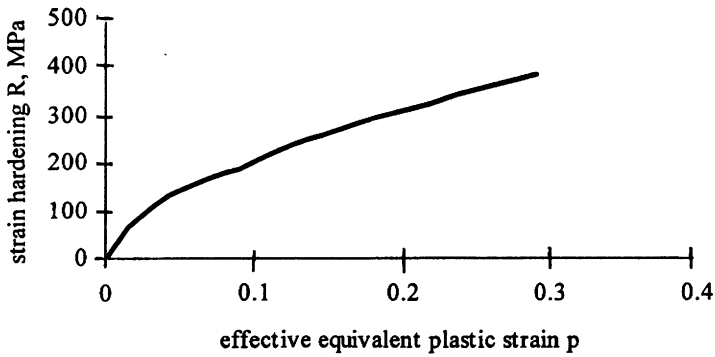

Figure 4. *Strain hardening curve* R(p).

Then, the plastic damage hardening B is derived from Equation (23) as

$$B = \{0.5(a_1^2 + \gamma a_2^2)\}^{1/2} \frac{\sigma^2}{E_0} - B_{0p} \tag{48}$$

where a_1 and a_2 can be expressed as:

$$a_1 = \frac{1 - 4\nu_0\mu + 2(1-\nu_0)\mu^2}{(1-D)^3} \quad a_2 = \frac{2\mu(1-\nu_0) - 2\nu_0}{(1-D)^2} \tag{49}$$

The overall plastic damage w_p is obtained from Equation (28)

$$w_p = \int dw = \int \left\{2\left[(dD)^2 + \frac{(d\mu)^2}{\gamma}\right]\right\}^{1/2} \tag{50}$$

Therefore, the curve of plastic damage hardening $B(w_p)$ can be determined with Equations (48) and (50) from measured values of true stress-true strain and the corresponding damage variables D and μ. The critical value of overall damage w_c is also determined with Equation (50) by the corresponding w_p to the final rupture point.

For the material AL 2024-T3, the 0.2% yield stress R_0 is 330 MPa, then the initial plastic damage threshold B_{0p} is calculated as 0.936 MPa with Equation (47) and the critical value of overall damage w_c is determined as 0.185with Equation (50). From Equations (48) and (50), the plastic damage hardening curve $B(w_p)$ is given in Figure 5.

5.4 Fatigue Damage Threshold B_{0f} and Damage Efficiency Factor α

The fatigue damage threshold B_{0f} is determined using the measured values of

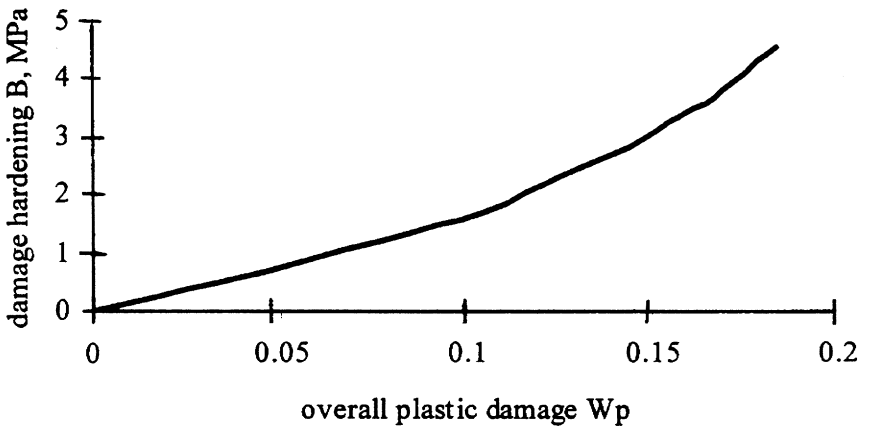

Figure 5. *Damage hardening curve* $B(w_p)$.

fatigue endurance limit. Under uniaxial tension-tension cyclic loading, the thermodynamic conjugate forces of fatigue damage variables D_f and μ_f in Equation (34) can be reduced as

$$\begin{aligned} Y_{Df} &= -\frac{a_1}{E_0}(\sigma - \sigma_{min})^2 \\ Y_{\mu f} &= -\frac{a_2}{E_0}(\sigma - \sigma_{min})^2 \end{aligned} \tag{51}$$

where a_1 and a_2 are expressed in Equation (49). Therefore, the fatigue damage threshold B_{0f} is derived from Equation (32) as

$$B_{0f} = \{0.5(a_1^2 + \gamma a_2^2)\}^{1/2} \frac{(\sigma_{1max} - \sigma_{1min})^2}{E_0} \tag{52}$$

where σ_{1min} and σ_{1max} are the minimum stress and the maximum stress corresponding to the fatigue endurance limit under a tension-tension cyclic load. If there is no plastic damage accumulation during the loading process (σ_{1min}, σ_{1max}), then Equation (52) becomes

$$B_{0f} = \{0.5(1 + 4\gamma\nu_0^2)\}^{1/2} \frac{(\sigma_{1max} - \sigma_{1min})^2}{E_0} \tag{53}$$

Under a tension-compression cyclic loading ($-\sigma_{2min}$, σ_{2max}), the parameter B_{0f} can be derived in a similar way with the concept of active stress defined in Equation (31) if there is no plastic damage accumulation during the loading process

$$B_{0f} = \{0.5(1 + 4\gamma v_0^2)\}^{1/2} \frac{(\sigma_{2max} + \alpha\sigma_{2min})^2}{E_0} \tag{54}$$

Comparing Equations (53) and (54), the damage efficiency factor α is derived as

$$\alpha = \frac{\sigma_{1max} - \sigma_{2max} - \sigma_{1min}}{\sigma_{2min}} \tag{55}$$

For the material AL 2024-T3, the fatigue endurance limit is defined as the fatigue strength corresponding to 5×10^7 cycles. The surface of fatigue endurance limit, like the yield surface, can be constructed in stress space. Under tension-tension loading, a fatigue endurance limit was measured at $\sigma_{1max} = 136$ MPa and $\sigma_{1min} = 0$ MPa. The fatigue damage threshold B_{0f} can then be determined as 0.159 MPa with Equation (53). Under tension-compression loading, two measured values of the fatigue endurance limit are (–47 MPa, 111 MPa) and (–100 MPa, 100 MPa). Therefore, the average damage efficiency factor α is given as 0.45 by Equation (55).

5.5 Fatigue Damage Constant K_0

This parameter is determined from the measured fatigue life under uniaxial cyclic loading. From Equations (36) and (38), if there is no plastic damage accumulation, the total overall damage in a cycle is

$$\Delta w_i(K_0) = \Delta w_{if}(K_0) = \int_{\sigma_c}^{\sigma_{max}} dw_{if} \tag{56}$$

Summing $\Delta w_i(K_0)$ up to the number of cycles N between 1 and N_f (the number of cycles to failure) leads to

$$w_c = \sum_{1}^{N_f} \Delta w_i(K_0) \tag{57}$$

Therefore, K_0 can be determined by numerically integrating Equation (57) from the measured value N_f corresponding to the applied cyclic loading (σ_{min},σ_{max}).

For the material AL 2024-T3, two uniaxial tension-tension loads, (60 MPa, 260 MPa) and (10 MPa, 260 MPa) respectively, are applied. The corresponding fatigue

lives are 301,000 cycles and 154,600 cycles. Then, the average fatigue damage constant K_0 can be determined as 761,000 MPa with Equation (57).

6. CONCLUSIONS

The following can be concluded from the present investigation:

1. A two-scalar damage model has been developed to characterize the fatigue damage accumulation and the plastic damage accumulation for a rate-independent material under fatigue loading.
2. The fatigue damage model is able to take into account the experimental observation that both the Young's modulus and the Poisson's ratio change during load application as demonstrated.
3. The ability of the model to characterize material behaviors has been separately verified under multiaxial loading conditions, including pure shear stress and biaxial stress conditions [24].
4. The model can be used to describe the effect of the hydrostatic stress on fatigue, as the damage accumulation is dependent upon the damage energy release rate that includes the hydrostatic stress effect.
5. The damage efficiency factor is introduced to take into account the difference between tension and compression in fatigue damage accumulation.
6. An experimental program to determine the material parameters of AL 2024-T4 is described. The measured parameters are summarized as:

$$E_0 = 74,300 \text{ MPa} \quad B_{0p} = 0.936 \text{ MPa} \quad \nu_0 = 0.34 \quad \alpha = 0.45 \quad \gamma = -0.4$$

$$K_0 = 761,000 \text{ MPa} \quad B_{0f} = 0.159 \text{ MPa} \quad R_0 = 330 \text{ MPa} \quad w_c = 0.185$$

The strain hardening and the damage hardening curves are respectively depicted in Figures 4 and 5.

7. The fatigue damage model has been implemented in ABAQUS through its user-defined subroutine UMAT. Applications of the model for crack initiation and propagation with FEM analysis in an engineering component will be the subject of future publications.

REFERENCES

1. Frost, N. E., K. J. Marsh and L. P. Pook. 1974. *Metal Fatigue,* Oxford University Press.
2. Sines, G. 1981. "Fatigue Criteria under Combined Stresses or Strain," *J. Engng. Mater. Technol.,* 13:82–90.
3. Miller, K. J. 1987. "The Behavior of Short Fatigue Cracks and Their Initiation Part 1—A Review of Two Recent Books; Part 2—A General Summary," *Fatigue Fract. Engng. Mater. Struct.,* 10:75–113.

4. Socie, D. 1987. "Multiaxial Fatigue Damage Assessment," *Low Cycle Fatigue and Elasto-Plastic Behaviour of Metals,* Elsevier Applied Science, pp. 465–472.
5. Tanaka, K. 1987. "Mechanisms and Mechanics of Short Fatigue Crack Propagation," *JSME International Journal Series,* 1, 30:1–13.
6. Coffin, L. F. 1988. "Some Perspectives on Future Directions in Low Cycle Fatigue," *Low Cycle Fatigue, ASTM STP 942,* Philadelphia, pp. 5–14.
7. Leese, G. E. 1988. "Engineering Significance of Recent Multiaxial Research," *Low Cycle Fatigue, ASTM STP 942,* Philadelphia, pp. 861–873.
8. Manson, S. S. 1988. "Future Directions for Low Cycle Fatigue," *Low Cycle Fatigue, ASTM STP 942,* Philadelphia, pp. 15–39.
9. Tanaka, K. 1989. "Mechanics and Micromechanics of Fatigue Crack Propagation," *Fracture Mechanics: Perspectives and Directions, ASTM STP 1020,* pp. 151–183.
10. Lemaitre, J. and J. L. Chaboche. 1990. *Mechanics of Solid Materials,* Cambridge University Press.
11. Miller, M. P., D. L. McDowell and R. L. T. Oehmke. 1992. "A Creep-Fatigue-Oxidation Microcrack Propagation Model for Thermomechanical Fatigue," *J. Engng. Mater. Technol.,* 114:282–288.
12. Kachanov, L. M. 1958. "On Creep Rupture Time," *Izv. Acad. Nauk SSSR, Otd. Techn. Nauk,* 8:26–31.
13. Krajcinovic, D. and G. U. Fonseka. 1981. "The Continuous Damage Mechanics of Brittle Materials, Parts I and II," *J. Appl. Mech.,* 48:809–824.
14. Chow, C. L. and J. Wang. 1987. "An Anisotropic Theory of Continuum Damage Mechanics for Ductile Fracture," *Engng. Fract. Mech.,* 27:547–558.
15. Ju, J. W. 1989. "On Energy Based Coupled Elastoplastic Damage Theories: Constitutive Modeling and Computational Aspect," *Int. J. Solids Struct.,* 25:805–833.
16. Chow, C. L. and Y. Wei. 1991. "A Model of Continuum Damage Mechanics for Fatigue Fracture," *Int. J. of Fracture,* 50:301–316.
17. Wei, Y., C. L. Chow and B. J. Duggan. 1993. "A Damage Model of Fatigue Analysis for Alloy AL 2024-T3," *Advances in Engineering Plasticity and Its Applications,* Elsevier, pp. 363–370.
18. Hansen, N. R. and H. L. Schreyer. 1994. "A Thermodynamically Consistent Framework for Theories of Elastoplasticity Coupled with Damage," *Int. J. Solids Struct.,* 31:359–389.
19. Hayakawa, K. and S. Murakami. 1997. "Thermodynamical Modeling of Elastic-Plastic Damage and Experimental Validation of Damage Potential," *Int. J. Damage Mech.,* 6:333–363.
20. Lemaitre, J. and J. L. Chaboche. 1978. "Aspects Phenomenologiques de la Rupture Par Endamagement," *J. Mec. Appl.,* 2:317.
21. Chaboche, J. L. and P. M. Lesne. 1988. "A Non-Linear Continuous Fatigue Damage Model," *Fatigue Fract. Engng. Mater. Struct.,* 11:1.
22. Cordebois, J. P. and F. Sidoroff. 1982. "Damage Induced Elastic Anisotropy," *Mechanical Behaviour of Anisotropic Solids,* Martinus Nijhoff, pp. 761–774.
23. Lu, T. J. and C. L. Chow. 1990. "On Constitutive Equations of Inelastic Solids with Anisotropic Damage," *Theoretical and Applied Fracture Mechanics,* 14:187–218.
24. Fang, H. E., C. L. Chow and Y. Wei. 1998. "Characteristics of Shear Damage for 60Sn-40Pb Solder Material," *Modeling and Simulation Based Engineering,* Tech Science Press, 2:1078–1083.